ENVIRONMENTAL RESEARCH
LETTERS

LETTER • **OPEN ACCESS**

Probabilistic explanation for episodic ecological events

To cite this article: Husile Bai *et al* 2024 *Environ. Res. Lett.* **19** 114004

IOP Publishing Environ. Res. Lett. 19 (2024) 114004 https://doi.org/10.1088/1748-9326/ad78ee

ENVIRONMENTAL RESEARCH
LETTERS

RECEIVED
31 March 2024

REVISED
29 August 2024

ACCEPTED FOR PUBLICATION
10 September 2024

PUBLISHED
20 September 2024

LETTER

Probabilistic explanation for episodic ecological events

Husile Bai[1,*], **Olivia Mondlock**[2], **Courtenay Strong**[2], **Jalene M LaMontagne**[3,4,5] and **Benjamin Zuckerberg**[6]

[1] Department of Earth and Environmental Sciences, Vanderbilt University, 2201 West End Ave, Nashville, TN 37235, States of America
[2] Department of Atmospheric Sciences, University of Utah, 135 S 1460 E, Salt Lake City, UT 84112, United States of America
[3] Department of Biology, University of Missouri—St. Louis, 1 University Blvd, St. Louis, MO 63121, United States of America
[4] Whitney R. Harris World Ecology Center, University of Missouri—St. Louis, 1 University Blvd, St. Louis, MO 63121, United States of America
[5] Science and Conservation Division, Missouri Botanical Garden, 4344 Shaw Blvd, St. Louis, MO 63110, United States of America
[6] Department of Forest and Wildlife Ecology, University of Wisconsin-Madison, 1630 Linden Drive, Madison, WI 53706, United States of America
[*] Author to whom any correspondence should be addressed.

E-mail: husile.bai@vanderbilt.edu, oliviamondlock@gmail.com, court.strong@utah.edu, jalene.lamontagne@umsl.edu and bzuckerberg@wisc.edu

Keywords: climate variability, episodic ecological events, probabilistic explanation

Abstract

Climate associated ecological phenomena that occur approximately once per decade suggest the influence of decadal climate oscillations. However, the consistency and origins of such climate patterns in the Atlantic and Pacific regions is currently under debate. Here, we propose a probabilistic explanation for episodic ecological events based on the likelihood of multiple climate patterns converging in a particular phase combination. To illustrate, we apply this model to continental scale facultative migration of seed-eating finches out of the boreal forest. This *irruption* phenomenon is triggered by seed crop failures stemming from two weakly correlated climate patterns occurring simultaneously in their positive phases—the North Atlantic Oscillation (NAO) and the North Pacific Oscillation (NPO). The joint probability of NAO and NPO both being positive (above upper tercile) is about $(1/3)^2 \approx 0.11$, illustrating a simple probabilistic explanation for quasi-decadal finch irruption and potentially other episodic ecological events in regions affected by multiple climate modes.

1. Introduction

Episodic ecological events are recognized as potentially high-impact drivers of dynamics in a broad range of settings [1–3]. Climate-triggered events occurring approximately once per decade suggest the presence of decadal climate oscillations, but recent research is casting doubt on the physical robustness of such climate patterns. For example, the Pacific Decadal Oscillation (PDO) is no longer viewed as an intrinsic oceanic mode, but is instead interpreted as a combination of different physical processes including remote tropical forcing and local atmosphere-ocean interactions [4]. As another prominent example, the Atlantic Multidecadal Oscillation (AMO) was previously believed to be a coherent internal oscillation of the climate system, but is now understood to stem from competing time-varying effects of anthropogenic greenhouse gases and sulfate aerosols [5–7].

The preceding motivates a hypothesis to explain episodic ecological events that allows for, but does not rely on the existence of decadal climate oscillations. To illustrate, we examine continental-scale facultative migration of pine siskins (*Spinus pinus*) out of the boreal forest, a phenomenon referred to as irruption. This species exhibits mass migration of large numbers of individuals in response to synchronized geographic fluctuations in seed production, moving away from regions with anomalously low seed production [8, 9]. The irruption of pine siskins southward out of the boreal forest is referred to as the North–South Mode (NSM) (figure 1(a)), where the NSM is defined as the leading principal component of pine siskin density and accounts for 40% of the total variance [8].

Notably, the NSM captures only two irruptions in the past three decades, indicating a quasi-decadal periodicity (figure 1(b)). The precipitation and temperature anomalies conducive to low seed production appear during late spring to early summer (May–June) in the previous year over the Canadian boreal forest and Great Lakes region [8], but the climate modes that cause these anomalies to occur only about once per decade are unknown. Potentially relevant patterns active in this region include the North American Dipole (NAD) recently linked to a West-East Mode of pine siskin irruption [10, 11], along with the North Pacific Oscillation (NPO) [12] and North Atlantic Oscillation (NAO) [13], but these pressure oscillations are largely interannual in nature and lack significant energy on decadal time scales [14, 15]. This leaves open the important question of what triggers intermittent, high-impact events like irruption, and what climate patterns should therefore be studied to predict their future changes.

2. Materials and methods

The significance of correlations and anomalies was assessed through t-tests with an assumption of one degree of freedom per year. Patterns of variability were examined using principal component analysis (PCA), alternatively referred to as empirical orthogonal function (EOF) analysis [16].

2.1. Bird data

The magnitude and periodicity of bird irruptions were analyzed using observations collected during Project FeederWatch (PFW) [17]. Bird (e.g. pine siskin) counts consist of a 2-day observation period separated by 5 days and begin on the second Saturday in November and run for 21 weeks during the winter. We totaled the bird counts over that period for each site and year in which the collection period ended (e.g. FeederWatch year 1989 corresponds to November 1988 through April 1989). PFW has been collecting data since 1989 and over 25 000 participants regularly enlist annually across the United States and Canada [18, 19]. We chose pine siskins as focal species, because they are one of the most visible and widespread North American seed-eating birds and they also engage in irruptive movements [20]. Data for 1989–2021 were analyzed to obtain the North-South spatial pattern and index following the methods detailed in our prior work [8, 10, 21]. The temporal pattern of pine siskin's irruption was displayed by plotting the standardized (z-score) principal component versus year, indicating the sign and magnitude of the mode. Here, the time series of the leading principal component (PC1) was determined as the North-South mode (NSM) of bird irruption (figure 1(b)) and referred to as the NSM index ($\mathrm{NSM_i}$).

2.2. Seed data

Data on annual conifer seed production were primarily obtained from the MASTREE+ mast-seeding database [22], and we extracted data focusing on Canada and the continental United States; the analysis period is 1987–2021, overlapping the bird records. We synthesized data from the family Pinaceae including *Abies spp.*, *Picea spp.*, and *Tsuga spp.* ($n = 711$ time series) to investigate the lagged correlation between bird NSM irruption and the atmospheric circulation patterns. To ensure robust analysis, only time series with a minimum length of six years were included, and all data were standardized to a scale of 0–100 prior to analysis [21].

2.3. Climate data

For analysis of historical atmospheric variability, we used reanalysis data from 1940 to 2022 for monthly averaged 300 hPa geopotential height (Z_{300}) and sea level pressure (SLP) from the European Centre for Medium Range Weather Forecasts (ECMWF) Reanalysis (ERA5) on a 30 km grid [23]. The NAR index was developed by projecting May—June Z_{300} anomalies onto the pattern shown in figure A1, which is the lagged correlation between bird NSM index and ERA5 May—June Z_{300} over the domain of $35^\circ - 65^\circ$ N, $240^\circ - 290^\circ$ E (i.e. Z_{300} data are from the summer preceding the NSM index). For the conventional NAO and NPO indices [12, 24], we used the domains indicated by red boxes in figures A2(a) and (b) in supplementary information, respectively, but we calculated the indices for the May—June period from 1940 to 2022 to ensure temporal overlap with our study time span.

2.4. Principal component analysis (PCA)

The variability patterns of bird density data and the atmospheric circulation data were examined through the application of principal component analysis (PCA), also known as empirical orthogonal function (EOF) analysis [16].

NSM was defined as in our prior work [8], but here extended to a longer time period. Specifically, the NSM is the leading principal component (PC1) of bird counts during the period from 1989 to 2021 [25]. The spatial pattern of the NSM is the first eigenvector of the spatial correlation matrix, illustrated by the correlation between bird counts and the NSM in figure 1(a). The associated index is the bird count data projected onto the NSM spatial patterns (blue curve in figure 1(b)).

All climate data were detrended prior to the analysis. The first two principal components of observed historical Z_{300} were derived from ERA5 data within the domain 35°–65°N, 170°–340°E, averaged over May–June for the years 1940–2022. The spatial patterns of these principal components corresponds to eigenvectors of the spatial correlation matrix (figures 3(b) and (c)). The time series of the principal

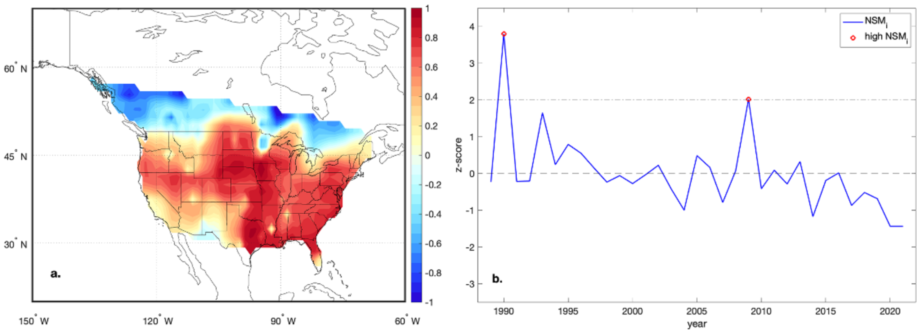

Figure 1. The North–South irruption mode (NSM) (a) NSM spatial pattern shown by the correlation between the NSM index (NSM$_i$) and and pine siskin counts, where the NSM$_i$ is the leading principal component of pine siskin counts, accounting for 40% of variance. (b) The NSM$_i$ time series corresponding to the analysis period 1989–2019, with red circles indicating irruption.

components were produced by projecting the climate data onto the spatial pattern of each principle component (blue curves, figures 3(e) and (f)).

3. Results

The first two columns in figure 2 illustrate a two-summer climate-masting sequence that is common over the boreal forest—a west-east dipole of masting anomalies [26] paired with a west-east dipole of atmospheric pressure referred to as the North Atlantic Dipole [10, 11]. This characteristic sequence features a summer of anomalously high pressure and masting over the eastern boreal forest (red shading, figures 2(a) and (d)) followed by a summer of the same over the western boreal forest (red shading, figures 2(b) and (e)). The NSM occurs in the winter after this west-east dipole is interrupted, meaning masting is simultaneously weak over both the western and eastern boreal forest (blue shading, figure 2(f)). The associated climate driver is a dipole of low pressure over the Gulf of Alaska paired with strong high pressure over the central boreal forest (dark blue and red shading, figure 2(c)), and the central question here focuses on why this NSM-triggering pattern occurs only about once per decade.

We developed an index to track the circulation pattern in figure 2(c), referred to as the North American Ridging (NAR) index (see section 2). The NAR index is significantly correlated with the NSM irruption index ($r > 0.63, p < 0.01$) during the overlapping period of 1989–2021 (figure 3(d)), and is extended to the longer period 1940–2022 to provide a more robust sample size for climate analysis. Positive values of the NAR correspond to higher than average atmospheric pressures over central Canada, visible as anomalously high 300 hPa geopotential heights (Z_{300}; red shading, figure 3(a)). This central Canadian ridging is associated with a positive NPO-like circulation pattern to the west over the gulf of Alaska, paired with a positive NAO-like pattern to the east around Greenland and the subtropical North Atlantic (figure 3(a)) (spatial patterns of positive NAO and NPO are shown for reference in figure A2).

The pattern in figure 3(a) can thus be interpreted as a superposition of positive NAO with positive NPO. To illustrate quantitatively, we use the first principal component (PC1) of Z_{300} to represent the NAO (figure 3(b)) and corresponding PC2 to represent the NPO (figure 3(c)), noting that these PC-based indices are significantly correlated with conventionally defined indices of the NAO ($r = 0.68, p < 0.01$; figure 3(e)) and NPO ($r = 0.48, p < 0.01$; 3(f)). Illustrating the concept of *climate mode superposition*, a linear combination of PC1 and PC2 accounts for more than 70% of the variance of the NAR index (figure A2(c)). As a key point, the NAO and NPO are uncorrelated ($r = -0.09$; $p = 0.41$). In a discrete time joint probability model, the joint probability of them simultaneously occurring in positive phase (above their upper terciles) is about $(1/3)^2 \approx 0.11$, meaning this is expected to occur on average about once per decade.

4. Discussion and conclusion

If an ecological event is infrequent but tends to recur at some interval (i.e. is intermittent or episodic), it may seem logical to seek or assume the existence of an oscillation at the same frequency in the climate system. A singular ecological event can be triggered by a climate extreme, which is rare by definition. However, recent work casts doubt on the physical mechanism of such low frequency oscillations [4–7], meaning that a complete explanation for such episodic ecological events should allow for, but not be reliant on, their existence.

Across the northern hemisphere, over 20 vertebrate species undergo high-amplitude oscillations in population numbers that exhibit 10 year cyclic dynamics [27, 28]. Many of these population cycles for northerly species, such as snowshoe hares (*Lepus americanus*) and ruffed grouse (*Bonasa umbellus*), are some of the most widely recognized examples of population dynamics in ecology [29–31]. The underlying

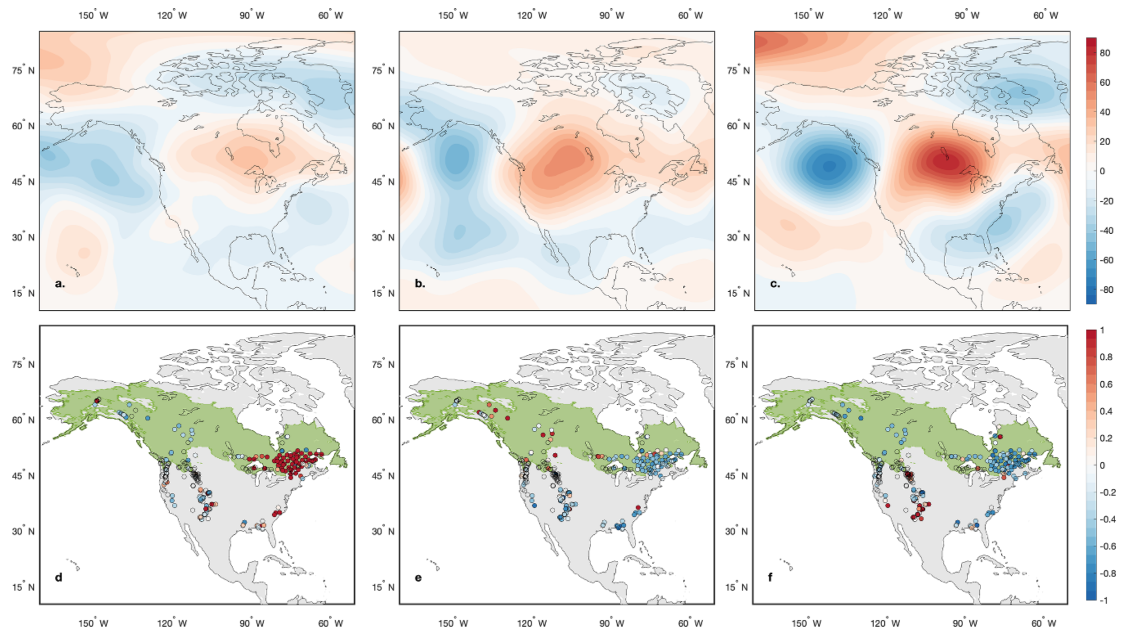

Figure 2. Composite atmospheric conditions and mast seeding preceding irruption. For high values of the North-South Mode irruption index ($\text{NSM}_\text{i} \geqslant 2.0$; red circle in figure 1(b)), composite anomalies of the 300 hPa geopotential height (Z_{300}) in (a) three summers prior to irruption (Y_{-3}), (b) two summers prior to irruption (Y_{-2}), and (c) one summer prior to irruption (Y_{-1}). (d)–(e) Similar as (a)–(c) but for the composite anomalies of the standardized masting index (d) Y_{-2}, (e) Y_{-1}, and (f) during the summer immediately before irruption (Y_0). Green shading indicates the boreal forest region. The analysis period corresponds to the overlap of the masting data with the pine siskin record, 1989–2021.

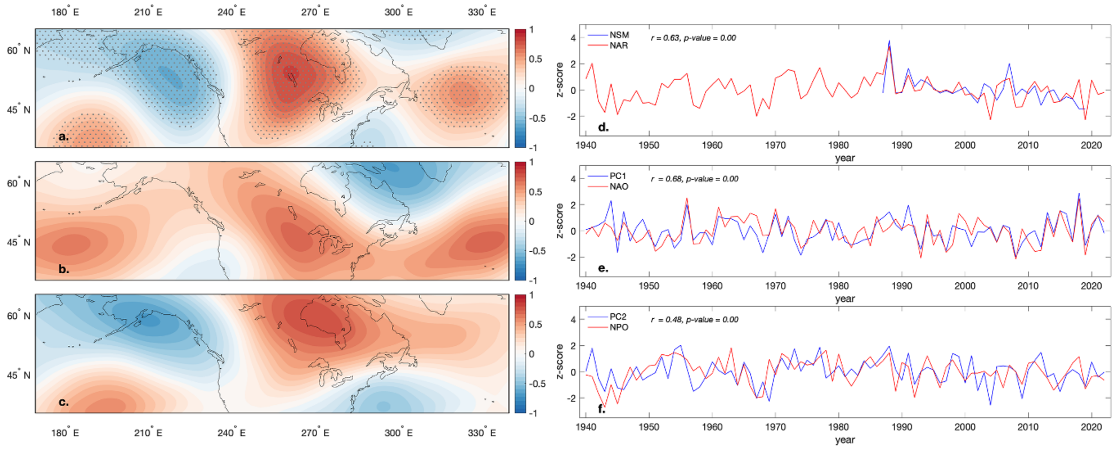

Figure 3. Climate mode superposition (a) The circulation pattern that precedes irruption, shown as the correlation of the North American Ridge index (NAR) with ERA5 May–June 300 hPa geopotential height (Z_{300}). Stippling indicates statistical significance at the 95% confidence level. (b) The circulation pattern of the leading principal component (PC1) of the Z_{300} over the NAR domain. (c) As in (b), but for the second principal component (PC2). (d) Time series indices of the NSM irruption index and North American Ridge (NAR) index. (e) Time series of PC1 and North Atlantic Oscillation (NAO) index, and (f) time series of PC2 and North Pacific Oscillation (NPO) index. The analysis period for the NAR and PCA is 1940–2022.

cause of these population cycles has been the subject of much debate, and although the tri-trophic interaction of food resources-prey-predators is traditionally considered the primary mechanism [32], climate variability is a critical component producing and sustaining the periodicity of population cycles [33, 34]. For example, modes of climate variability are critical for explaining the cyclic and time-lagged interactions between snowshoe hare and their primary predator, Canada lynx (*Lynx canadensis*), by mediating winter conditions [33]. Like the irruption dynamics of pine siskins and other boreal birds, it is possible that multiple climate patterns converge in a phase combination that entrain some of the most classical examples of population cycles in ecology.

The straightforward consideration of joint probabilities presented here explains how episodic ecological events can be triggered without requiring the existence of intrinsic decadal climate oscillations. In this probabilistic explanation for episodic ecological events, quasi-decadal occurrence stems from the likelihood of two or more climate patterns converging in a particular phase combination. This was illustrated by examining how convergence of positive NAO and NPO drives continental-scale facultative migration of seed-eating finches southward out of the boreal forest, but the model can apply more broadly because most regions are affected by multiple climate modes.

In the irruption example presented here, the event trigger was NAO and NPO both being positive (above upper tercile), yielding a likelihood consistent with decadal periodicity $[(1/3)^2 \approx 0.1]$. More generally, any phase combination for any two independent indices (one negative while other is neutral, both neutral, both negative, etc) has the same likelihood which is consistent with approximately decadal occurrence. For three independent indices, the likelihood of any particular phase combination reduces to $(1/3)^3 \approx 0.04$, corresponding to on average one event every 27 years.

The two patterns considered here (NAO and NPO) happened to lack strong correlation ($r = -0.09$; $p = 0.41$), which is not uncommon for climate modes detected using methods like principal components analysis. However, our approach to understanding periodicity can accommodate more elaborate joint probability scenarios. For example, one or more of the modes of variability considered could be influenced by a third mode such as the El Niño Southern Oscillation [35]. We can also consider, for example, two indices that are strongly positively correlated. If the ecological event is triggered by both occurring in the same phase, the likelihood could be closer to 1/3, meaning the event is expected every three years on average; if the event is triggered by the indices occurring in opposite phases, the likelihood could be closer to zero, rendering the event rare or singular.

Data availability statement

The mast-seeding datasets used for the study are available in the Dryad repository (https://datadryad.org/stash). The FeederWatch bird count observations used in this project are available from the Cornell Lab of Ornithology (https://www.birds.cornell.edu/home). Climate data are available from the European Centre for Medium Range Weather Forecasts (https://www.ecmwf.int/en/forecasts/dataset/ecmwf-reanalysis-v5).

Acknowledgments

This work is supported by National Science Foundation Grant Nos. 1926221, 1926428 and 1926341. We thank the University of Utah Center of High Performance Computing (CHPC) for computational resources and computer-support services.

Author contributions

HB and CS conceived the study, computational analyses were performed by HB and OM, and all authors contributed to writing.

Conflict of interest

The authors declare no competing interests.

Appendix. Supporting figures

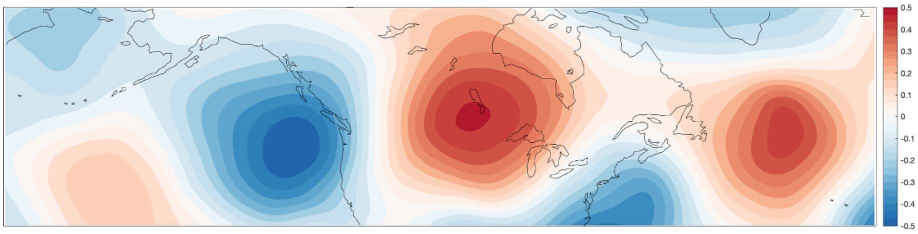

Figure A1. Correlation pattern. Lagged one-year correlation of Z_{300} with NSM index, which is used to defined the North American Ridging index (NAR; red curve in figure 3(d)).

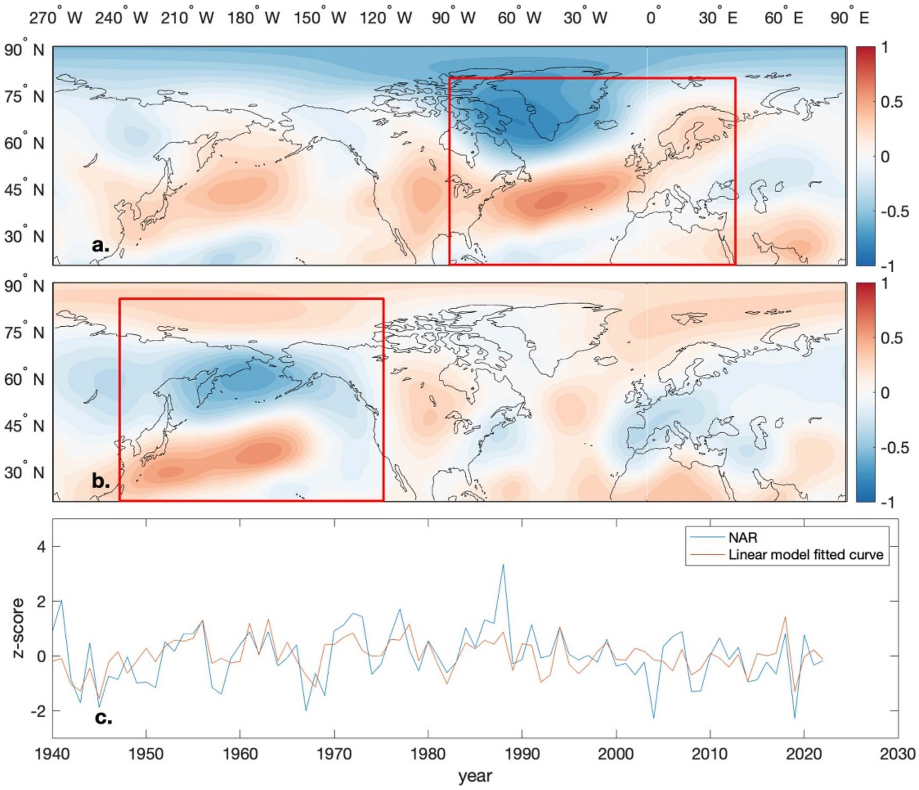

Figure A2. Pattern match between the North Atlantic Oscillation (NAO), North Pacific Oscillation (NPO), and bird's NSM relevant atmospheric circulation—North American Ridging (NAR). The correlation of Z_{300} with the (a) NAO pattern and (b) NPO pattern, where the red box indicates the analysis region for each index. (c) Time series for the NAR index and linear model of the NAR using the NAO and NPO as predictors.

ORCID iD

Husile Bai https://orcid.org/0009-0008-1399-9569

References

[1] Boero F 1996 Episodic events: their relevance to ecology and evolution *Mar. Ecol.* **17** 237–50

[2] Pederson N, Dyer J M, McEwan R W, Hessl A E, Mock C J, Orwig D A, Rieder H E and Cook B I 2014 The legacy of episodic climatic events in shaping temperate, broadleaf forests *Ecol. Monogr.* **84** 599–620

[3] Ummenhofer C C and Meehl G A 2017 Extreme weather and climate events with ecological relevance: a review *Phil. Trans. R. Soc.* B **372** 20160135

[4] Newman M *et al* 2016 The pacific decadal oscillation, revisited *J. Clim.* **29** 4399–427

[5] Mann M E, Steinman B A and Miller S K 2014 On forced temperature changes, internal variability and the AMO *Geophys. Res. Lett.* **41** 3211–9

[6] Clement A, Bellomo K, Murphy L N, Cane M A, Mauritsen T, Rädel G and Stevens B 2015 The Atlantic Multidecadal Oscillation without a role for ocean circulation *Science* **350** 320–4

[7] Mann M E, Steinman B A, Brouillette D J and Miller S K 2021 Multidecadal climate oscillations during the past millennium driven by volcanic forcing *Science* **371** 1014–9

[8] Strong C, Zuckerberg B, Betancourt J L and Koenig W D 2015 Climatic dipoles drive two principal modes of north american boreal bird irruption *Proc. Natl Acad. Sci.* **112** 2795–802

[9] Zuckerberg B, Strong C, LaMontagne J M, George S S, Betancourt J L and Koenig W D 2020 Climate dipoles as continental drivers of plant and animal populations *Trends Ecol. Evol.* **35** 440–53

[10] Bai H, Strong C and Zuckerberg B 2023 Drivers of an ecologically relevant summer north american dipole *J. Clim.* **36** 2387–99

[11] Bai H and Strong C 2023 Atmospheric modeling study on convection-triggered teleconnections driving the summer north american dipole *J. Clim.* **36** 6991–7003

[12] Linkin M E and Nigam S 2008 The north pacific oscillation–west pacific teleconnection pattern: mature-phase structure and winter impacts *J. Clim.* **21** 1979–97

[13] Hurrell J W 1995 Decadal trends in the north atlantic oscillation: regional temperatures and precipitation *Science* **269** 676–9

[14] Feldstein S B 2000 The timescale, power spectra and climate noise properties of teleconnection patterns *J. Clim.* **13** 4430–40

[15] Fernández I, Hernández C N and Pacheco J M 2003 Is the north atlantic oscillation just a pink noise? *Physica* A **323** 705–14

[16] Hannachi A, Jolliffe I T and Stephenson D B 2007 Empirical orthogonal functions and related techniques in atmospheric science: a review *Int. J. Climatol.* **27** 1119–52

[17] Bonter D N and Hochachka W M 2009 A citizen science approach to ornithological research: twenty years of watching backyard birds *Proc. 4th Int. Partners in Flight Conf.: Tundra to Tropics* vol 4 pp 453–8

[18] Zuckerberg B, Bonter D N, Hochachka W M, Koenig W D, DeGaetano A T and Dickinson J L 2011 Climatic constraints on wintering bird distributions are modified by urbanization and weather *J. Anim.* **80** 403–13

[19] Zuckerberg B, Desrochers A, Hochachka W M, Fink D, Koenig W D and Dickinson J L 2012 Overlapping landscapes: a persistent, but misdirected concern when collecting and analyzing ecological data *J. Wildlife Manage.* **76** 1072–80

[20] Watts H E, Robart A R, Chopra J K, Asinas C E, Hahn T P and Ramenofsky M 2017 Seasonal expression of migratory behavior in a facultative migrant, the pine siskin *Behav. Ecol. Sociobiol.* **71** 1–12

[21] Bai H, Strong C, LaMontagne J M, Widick I V and Zuckerberg B 2024 A north american climate-masting-irruption teleconnection and its change under future climate *Sci. Total Environ.* **948** 174473

[22] Hacket-Pain A *et al* 2022 Mastree+: time-series of plant reproductive effort from six continents *Glob. Change Biol.* **28** 3066–82

[23] Hersbach H, Bell B, Berrisford P, Hirahara S, Horányi A, Muñoz-Sabater J, Nicolas J, Peubey C, Radu R and Schepers D 2020 The ERA5 global reanalysis *Q. Meteorol. Soc.* **146** 1999–2049

[24] Chen W Y and Dool H V 2003 Sensitivity of teleconnection patterns to the sign of their primary action center *Mon. Weather Rev.* **131** 2885–99

[25] Bai H 2022 Teleconnection mechanisms associated with ecologically-relevant climate dipoles *PhD Thesis* University of Utah, 201 Presidents' Cir, Salt Lake City, UT 84112 (available at: www.proquest.com/docview/2778199984)

[26] LaMontagne J M, Pearse I S, Greene D F and Koenig W D Mast seeding patterns are asynchronous at a continental scale *Nat. Plants* **6** 460–5

[27] Keith L B and Cary J R 1991 Mustelid, squirrel and porcupine population trends during a snowshoe hare cycle *J. Mammal.* **72** 373–8

[28] Ims R A, Henden J-A and Killengreen S T 2008 Collapsing population cycles *Trends Ecol. Evol.* **23** 79–86

[29] Keith L B and Windberg L A 1978 A demographic analysis of the snowshoe hare cycle *Wildlife Monogr.* **58** 3–70 (available at: http://www.jstor.org/stable/3830596)

[30] Boutin S *et al* 1995 Population changes of the vertebrate community during a snowshoe hare cycle in canada's boreal forest *Oikos* **74** 69–80

[31] Krebs C J, Boutin S, Boonstra R, Sinclair A R E, Smith J N M, Dale M R T, Martin K and Turkington R 1995 Impact of food and predation on the snowshoe hare cycle *Science* **269** 1112–5

[32] Abdala-Roberts L *et al* 2019 Tri-trophic interactions: bridging species, communities and ecosystems *Ecol. Lett.* **22** 2151–67

[33] Yan C, Stenseth N C, Krebs C J and Zhang Z 2013 Linking climate change to population cycles of hares and LYNX *Glob. Change Biol.* **19** 3263–71

[34] Pomara L Y and Zuckerberg B 2017 Climate variability drives population cycling and synchrony *Divers. Distrib.* **23** 421–34

[35] Zhang W, ang Z, Stuecker M F, Turner A G, Jin F-F, Geng X Impact of ENSO longitudinal position on teleconnections to the NAO *Clim. Dyn.* **52** 257–74